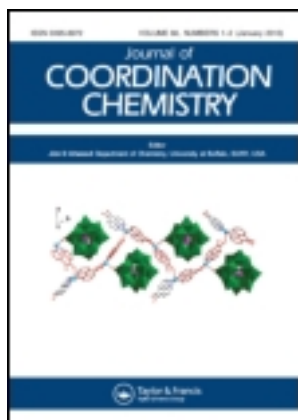


This article was downloaded by: [Renmin University of China]

On: 13 October 2013, At: 10:48

Publisher: Taylor & Francis

Informa Ltd Registered in England and Wales Registered Number: 1072954 Registered office: Mortimer House, 37-41 Mortimer Street, London W1T 3JH, UK



Journal of Coordination Chemistry

Publication details, including instructions for authors and subscription information:

<http://www.tandfonline.com/loi/gcoo20>

Synthesis, structure, and magnetic properties of two dimer paddle-wheel Cu^{II} toluate complexes with nitronyl nitroxide radicals

Jie Zhou^a, Lin Du^a, Zongze Li^a, Yongfeng Qiao^a, Jing Liu^a,
Minrong Zhu^a, Peng Chen^a & Qihua Zhao^a

^a Key Laboratory of Medicinal Chemistry for Natural Resource Education Ministry, Department of Chemistry, Yunnan University, Kunming, China

Published online: 03 Jun 2013.

To cite this article: Jie Zhou, Lin Du, Zongze Li, Yongfeng Qiao, Jing Liu, Minrong Zhu, Peng Chen & Qihua Zhao (2013) Synthesis, structure, and magnetic properties of two dimer paddle-wheel Cu^{II} toluate complexes with nitronyl nitroxide radicals, *Journal of Coordination Chemistry*, 66:12, 2166-2177, DOI: [10.1080/00958972.2013.800485](https://doi.org/10.1080/00958972.2013.800485)

To link to this article: <http://dx.doi.org/10.1080/00958972.2013.800485>

PLEASE SCROLL DOWN FOR ARTICLE

Taylor & Francis makes every effort to ensure the accuracy of all the information (the "Content") contained in the publications on our platform. However, Taylor & Francis, our agents, and our licensors make no representations or warranties whatsoever as to the accuracy, completeness, or suitability for any purpose of the Content. Any opinions and views expressed in this publication are the opinions and views of the authors, and are not the views of or endorsed by Taylor & Francis. The accuracy of the Content should not be relied upon and should be independently verified with primary sources of information. Taylor and Francis shall not be liable for any losses, actions, claims, proceedings, demands, costs, expenses, damages, and other liabilities whatsoever or howsoever caused arising directly or indirectly in connection with, in relation to or arising out of the use of the Content.

This article may be used for research, teaching, and private study purposes. Any substantial or systematic reproduction, redistribution, reselling, loan, sub-licensing, systematic supply, or distribution in any form to anyone is expressly forbidden. Terms &

Conditions of access and use can be found at <http://www.tandfonline.com/page/terms-and-conditions>

Synthesis, structure, and magnetic properties of two dimer paddle-wheel Cu^{II} toluate complexes with nitronyl nitroxide radicals

JIE ZHOU†, LIN DU†, ZONGZE LI, YONGFENG QIAO, JING LIU, MINRONG ZHU, PENG CHEN and QIHUA ZHAO*

Key Laboratory of Medicinal Chemistry for Natural Resource Education Ministry,
Department of Chemistry, Yunnan University, Kunming, China

(Received 5 November 2012; in final form 8 March 2013)

Two new paddle-wheel dimeric copper complexes, [Cu₂(4-MePhCOO)₄(NITmPy)₂] (**1**) and [Cu₂(3-MePhCOO)₄(NITmPy)₂] (**2**) (NITmPy = 2-(3-pyridyl)-4,4,5,5-tetramethyl-4,5-dihydro-1H-imidazolyl-1-oxyl-3-oxide), were synthesized by reaction of copper toluate and NITmPy. Single crystal X-ray analyses revealed that both complexes are symmetrical dimers. Cu with four deprotonated methylbenzoate bridging ligands form a paddle-wheel core and pyridyl nitrogen of radical ligands at the apical position. Based on the Cu–Cu axis of **1** and **2**, we exploited the steric constraints of the methyl groups and induced the paddle-wheel. Two magnetic exchange pathways with strong antiferromagnetic interaction between dimeric Cu^{II} ions and weak antiferromagnetic interaction between NITmPy ligands exist in the complexes. IR and powder X-ray diffraction of the complexes were also studied.

Keywords: Magnetic properties; Nitronyl nitroxide radicals; Paddle-wheel complexes; Toluic

1. Introduction

Carboxylates are widely used as bridging ligands in design and synthesis of paddle-wheel dimer metal carboxylate adducts, formulated as [M₂(RCOO)₄L₂], where L usually represents the Lewis base located at the axial position and the carboxylates are bridging on the equatorial position. By changing R and L, numerous zero-dimensional (0-D) to three-dimensional (3-D) paddle-wheel compounds can be synthesized [1–7]. Design of esthetic complexes and molecular assemblies that exhibit spontaneous magnetization are of interest to the magneto structural correlations [8–10]. Much effort has been exerted to clarify magnetic exchange interaction that occurs in paddle-wheel complexes. Interaction between the two metal ions of a paddle-wheel is generally antiferromagnetic regardless of the substituents R and apical ligands L; the antiferromagnetic interaction tends to increase as either L or R becomes a stronger electron donor [11–13].

*Corresponding author. Email: qhzhao@ynu.edu.cn

†Contributed equally to this work.

Stable organic radicals that can act as paramagnetic carriers and magnetic couplers have been widely used as molecular units in the metal-radical approach to molecular magnetic complexes [14–17]. Nitronyl nitroxide radicals can easily be chemically modified by varying R substituents which are capable of coordinating with the metal ions; many functionalized nitronyl nitroxide radicals have been synthesized such as pyridyl-, imidazolyl-, and carboxyl-substituted nitronyl nitroxides [18–22]. Thus, coordination abilities of the radicals which are limited by the weak basic nature of the nitroxide are increased [23]. Among the functionalized nitroxide radical ligands, pyridyl-substituted nitroxide radicals are the most extensively used to induce coupling due to their donor nitrogen [13, 24]. Copper(II) complexes are significant in the study of molecular magnets [25, 26].

Based on the above premises, we reacted copper *p*-toluate and copper *m*-toluate with the nitronyl nitroxide radicals in methanol and dichloromethane solutions and obtained two dimeric copper complexes, [Cu₂(4-MePhCOO)₄(NITmPy)₂] (**1**) and [Cu₂(3-MePhCOO)₄(NITmPy)₂] (**2**). In the complexes, two copper ions are bridged by four toluate ligands. Two radical molecules are coordinated to copper through pyridine N on the apical position. Based on the Cu–Cu axis of **1** and **2**, we exploited the steric constraints of the methyl groups and induced the paddle-wheel to run. To the best of our knowledge, such observation on copper paddle-wheel complexes with radicals has not been previously reported. In this paper, we report the crystal structure and magnetic properties of **1** and **2**.

2. Experimental

2.1. General

All chemicals used were of reagent grade and used without purification. The carbon, hydrogen, and nitrogen contents were acquired with a Vario-EL III element analyzer. Infrared spectra were recorded with a SHIMADZU IR prestige-21 FTIR-8400S spectrometer from 4000–400 cm⁻¹ as KBr pellets. The phase purities of the samples were investigated by powder X-ray diffraction (PXRD) measurements on a Bruker D8-Advance diffractometer equipped with Cu-K α radiation ($\lambda = 1.5406 \text{ \AA}$) at a scan speed of 1 °/min. Simulation of the PXRD patterns were obtained using single-crystal data and were processed by the Mercury v1.4 program available free of charge through the Internet at <http://www.iucr.org>. The crystal structures were determined by a Rigaku SCXmini diffractometer and the SHELXL-97 crystallographic software package. The temperature dependent magnetizations (*M* vs. *T*) (2–300 K) of **1** and **2** were measured by using a Quantum Design vibrating sample magnetometer in Physical Property Measurement System.

2.2. Preparation of **1** and **2**

2-(3-Pyridyl)-4,4,5,5-tetramethylimidazoline-1-oxyl-3-oxide (NITmPy) [14, 15] and copper *p*-toluate [27] were prepared according to methods described previously. Complex **1** was synthesized by adding a solution of NITmPy (0.1 mmol) in CH₂Cl₂ (10 mL) to a solution of copper *p*-toluate (0.1 mmol) in methanol (10 mL) dropwise. The mixture was stirred for 1 h at ambient temperature and then filtered. The clear blue filtrate was kept in the dark and was slowly evaporated at room temperature. A few weeks later, dark-blue crystals suitable for X-ray analysis were obtained. C₅₆H₆₀Cu₂N₆O₁₂ Calcd: C 59.20, H 5.32,

N 7.40; found: C 59.02, H 5.21, N 7.52. IR (KBr, cm^{-1}): 2986.27, 2928.24, 1622.13, 1563.78, 1404.07, 1323.20, 1209.73, 1169.95, 766.93, 697.38, 631.56, 461.29.

Complex **2** was synthesized in a manner similar to that of **1** replacing copper *p*-toluate with copper *m*-toluate. $\text{C}_{56}\text{H}_{60}\text{Cu}_2\text{N}_6\text{O}_{12}$ Calcd: C 59.20, H 5.32, N 7.40; found: C 59.11, H 5.41, N 7.26. IR data (KBr, cm^{-1}): 2986.27, 2923.15, 1625.72, 1587.71, 1400.45, 1321.00, 1212.37, 1131.99, 755.66, 687.87, 487.77.

2.3. Crystallographic data collection and refinement

Single crystal X-ray diffraction data were collected at 293 K on a Bruker Smart AXS CCD diffractometer with graphite-monochromated Mo- $K\alpha$ radiation ($\lambda = 0.71073 \text{ \AA}$). Absorption correction was performed by the multi-scan method. Empirical absorption corrections were carried out using SADABS. The structures were solved by direct methods and refined on F^2 by full-matrix least-squares using SHELXL-97. SHELXS-97 and SHELXL-97 programs were used for structure solution and refinement [28, 29]. All nonhydrogen atoms were refined with anisotropic displacement parameters. For **2**, the highest peak was 0.40 (0.4819, 0.0650, and 0.3507) [0.97 \AA from O2] and the deepest hole was -1.05 (0.4423, 0.0000, and 0.2409) [1.02 \AA from Cu1]. The collection parameters are shown in table 1. Selected bond distances and angles of **1** and **2** are listed in tables 2 and 3, respectively.

Table 1. Crystallographic data and structure refinement parameters for **1** and **2**.

Complex	1	2
Empirical formula	$\text{C}_{56}\text{H}_{60}\text{Cu}_2\text{N}_6\text{O}_{12}$	$\text{C}_{56}\text{H}_{60}\text{Cu}_2\text{N}_6\text{O}_{12}$
Crystal system	Triclinic	Monoclinic
Space group	$P\bar{1}$	$C2/m$
Formula weight	1136.20	1136.18
Wavelength	0.71073 \AA	0.71073 \AA
Crystal size	$0.23 \times 0.17 \times 0.12 \text{ mm}$	$0.26 \times 0.17 \times 0.12 \text{ mm}$
Unit cell dimensions	$a = 10.7932(9) \text{ \AA}$ $b = 13.3891(11) \text{ \AA}$ $c = 19.5436(16) \text{ \AA}$ $\alpha = 94.8570(10)^\circ$ $\beta = 95.5170(10)^\circ$ $\gamma = 95.3170(10)^\circ$	$a = 21.130(5) \text{ \AA}$ $b = 15.890(4) \text{ \AA}$ $c = 8.1389(18) \text{ \AA}$ $\alpha = 90^\circ$ $\beta = 96.861(3)^\circ$ $\gamma = 90^\circ$
Volume	$2786.6(4) \text{ \AA}^3$	$2713.1(11) \text{ \AA}^3$
Z	2	2
Calculated density	1.354 g cm^{-3}	1.391 g cm^{-3}
Absorption coefficient	0.829 mm^{-1}	0.851 mm^{-1}
θ range for data collection	$1.53\text{--}25.10^\circ$	$1.61\text{--}25.09^\circ$
Limiting indices	$-12 \leq h \leq 12$; $-15 \leq k \leq 157$; $-23 \leq l \leq 23$	$-25 \leq h \leq 24$; $-18 \leq k \leq 18$; $-6 \leq l \leq 9$
Data/restraints/parameters	9889/48/685	2511/0/190
Refinement method	Full-matrix least-squares on F^2	Full-matrix least-squares on F^2
Reflections collected/unique	22,440/9889 [R (int) = 0.0387]	7782/2511 [R (int) = 0.0904]
Completeness to theta = 25.00	99.7%	99.9%
Goodness-of-fit on F^2	1.025	1.032
Final R_1 , indices [$I > 2\sigma(I)$]	$R_1 = 0.0504$, $wR_2 = 0.1175$	$R_1 = 0.0694$, $wR_2 = 0.1534$
R indices (all data)	$R_1 = 0.0936$, $wR_2 = 0.1394$	$R_1 = 0.1189$, $wR_2 = 0.1844$
Largest diff. peak and hole	0.397 and -0.493 e\AA^{-3}	0.395 and -1.049 e\AA^{-3}

Table 2. Selected bond lengths (Å) and angles (°) for **1**.

Cu(1)–O(3)	1.974(2)	Cu(1)–O(4)	1.970(2)
Cu(1)–O(5)	1.965(3)	Cu(1)–O(6)	1.967(3)
Cu(1)–N(1)	2.197(3)	Cu(1)–Cu(1)a	2.6464(9)
O(1)–N(2)	1.267(5)	O(2)–N(3)	1.276(4)
Cu(2)–O(15)	1.973(2)	Cu(2)–O(16)	1.985(2)
Cu(2)–O(17)	1.956(3)	Cu(2)–O(18)	1.962(3)
Cu(2)–N(7)	2.150(3)	Cu(2)–Cu(3)b	2.6213(9)
O(13)–N(8)	1.259(6)	O(14)–N(9)	1.250(5)
O(5)–Cu(1)–O(4)	90.6(1)	O(5)–Cu(1)–O(3)	88.7(1)
O(4)–Cu(1)–O(6)	87.1(1)	O(3)–Cu(1)–O(6)	91.0(1)
O(4)–Cu(1)–O(3)	168.3(1)	O(5)–Cu(1)–O(6)	167.9(1)
O(5)–Cu(1)–N(1)	97.6(1)	O(4)–Cu(1)–N(1)	98.1(1)
O(3)–Cu(1)–N(1)	93.4(1)	O(6)–Cu(1)–N(1)	94.4(1)
O(5)–Cu(1)–Cu(1)a	85.50(8)	O(4)–Cu(1)–Cu(1)a	87.52(8)
O(3)–Cu(1)–Cu(1)a	80.84(7)	O(6)–Cu(1)–Cu(1)a	82.56(8)
N(1)–Cu(1)–Cu(1)a	173.43(8)	C(13)–O(3)–Cu(1)	127.0(2)
C(13)a–O(4)–Cu(1)	119.3(2)	C(21)–O(5)–Cu(1)	121.0(3)
C(21)a–O(6)–Cu(1)	124.9(3)	O(18)–Cu(2)–O(17)	168.7(1)
O(18)–Cu(2)–O(15)	89.8(1)	O(17)–Cu(2)–O(15)	87.8(1)
O(18)–Cu(2)–O(16)	90.3(1)	O(17)–Cu(2)–O(16)	89.7(1)
O(15)–Cu(2)–O(16)	168.5(1)	O(18)–Cu(2)–N(7)	89.2(1)
O(17)–Cu(2)–N(7)	101.9(1)	O(15)–Cu(2)–N(7)	96.8(1)
O(16)–Cu(2)–N(7)	94.6(1)	O(18)–Cu(2)–Cu(2)b	81.33(8)
O(17)–Cu(2)–Cu(2)b	81.33(8)	O(17)–Cu(2)–Cu(2)b	87.55(8)
O(15)–Cu(2)–Cu(2)b	87.41(8)	O(16)–Cu(2)–Cu(2)b	81.29(8)
N(7)–Cu(2)–Cu(2)b	169.69(9)	C(69)–O(15)–Cu(2)	119.9(2)

Symmetry codes: a: $-x+2, -y+2, -z$; b: $-x+1, -y, -z+1$.Table 3. Selected bond lengths (Å) and angles (°) for **2**.

Cu(1)–O(1)	1.967(3)	Cu(1)–O(2)a	1.953(3)
Cu(1)–O(2)b	1.953(3)	Cu(1)–O(1)c	1.967(3)
Cu(1)–N(1)	2.185(5)	Cu(1)–Cu(1)a	2.670(1)
O(5)–N(2)	1.260(8)	O(6)–N(3)	1.22(1)
O(2)a–Cu(1)–O(2)b	87.4(2)	O(2)a–Cu(1)–O(1)c	90.4(1)
O(2)b–Cu(1)–O(1)c	167.5(1)	O(2)a–Cu(1)–O(1)	167.5(1)
O(1)c–Cu(1)–O(1)	88.9(2)	O(2)a–Cu(1)–N(1)	101.6(1)
O(1)c–Cu(1)–N(1)	90.8(1)	O(2)a–Cu(1)–Cu(1)a	86.9(9)
O(1)c–Cu(1)–Cu(1)a	80.67(9)	N(1)–Cu(1)–Cu(1)a	168.0(1)
C(13)–O(1)–Cu(1)	126.7(3)	C(13)–O(2)–Cu(1)a	120.6(3)

Symmetry codes: a: $-x+1, -y, -z+1$; b: $-x+1, y, -z+1$; c: $x, -y, z$.

3. Results and discussion

3.1. Crystal structure analysis

Single crystal X-ray analysis revealed that **1** crystallizes in the triclinic space group $P\bar{1}$, whereas **2** has higher symmetry crystallizing in the monoclinic space group $C2/m$. The two complexes have the same stoichiometry and connectivity consisting of centrosymmetric dinuclear units. Each Cu^{II} has four oxygens from four different carboxylates in the equatorial position and two pyridyl nitrogens of the radicals apical. In a five-coordinate copper system, the geometry around Cu^{II} may be square-pyramidal or trigonal-bipyramidal depending on the geometric parameter τ ($\tau = (\beta - \alpha)/60$, where β is defined as the greater of

the basal angles and α is the remaining angle) [30]. For a perfectly square-pyramidal geometry, τ is equal to 0. However, the value becomes unity for ideal trigonal-bipyramidal geometry. The τ value is 0.007 for **1** and 0 for **2**, respectively, which indicates that the coordination geometry of the two complexes is square-pyramidal and thus, different from the trigonal-bipyramidal dimer (figures 1(a) and 1(b)) [10]. In **1**, the dimers have two different orientations in the crystal (figure 1(c)). The Cu–Cu distances are 2.6464(9) and 2.6213(9) Å, Cu–O distances range from 1.962(3) to 1.985(2) Å, and Cu–N distances are 2.150(3) and 2.197(3) Å. All values are comparable to those in the previously reported dimeric Cu^{II} complexes with nitronyl nitroxides [31–34]. In **2**, the Cu–Cu distance is 2.670(1) Å and Cu–N is 2.180(5) Å. Both values are larger than those of **1**, ascribed to the presence of *m*-methyl that increases the steric effect of *m*-toluic with NITmPy ligands. As a result, the average Cu–O distance (1.960 Å) is relatively shorter than that of **1** (1.969 Å).

Within the coordinated NITmPy of **1**, the imidazole is nearly planar and forms a dihedral angle of 14.36(4)° with the pyridine ring. In **2**, the imidazole and pyridine rings are nearly in the same plane, and the other distances and angles within the nitroxide group of both complexes are similar to those previously reported [31–34]. Both complexes have relatively short contacts between O of N–O of neighboring dimer molecules. The distances are 3.68 and 6.32 Å for **1** and 4.99 Å for **2** (figures 1(c) and 1(d)). These values were considered in the treatment of the experimental dependence magnetic susceptibility.

In **1**, based on the Cu–Cu axis (figure 2(a)), the four *p*-toluic acids that bridge two copper ions are approximately perpendicular. Moreover, two apical NITmPy ligands are nearly in one plane with two *p*-toluic acids. However, in **2**, four *m*-toluic acids are vertical to each other and NITmPy ligands split the angle made of *m*-toluic acids and form a dihedral angle of 45° and 42° (figure 2(b)). This arrangement reduces the energy of the system and enhances the stability of the molecules. Based on the Cu–Cu axis of **1** and **2**, we exploited the steric constraints of the methyl groups and induced the paddle-wheel to run. To the best of our knowledge, such observation on copper paddle-wheel complex with radicals has not been previously reported.

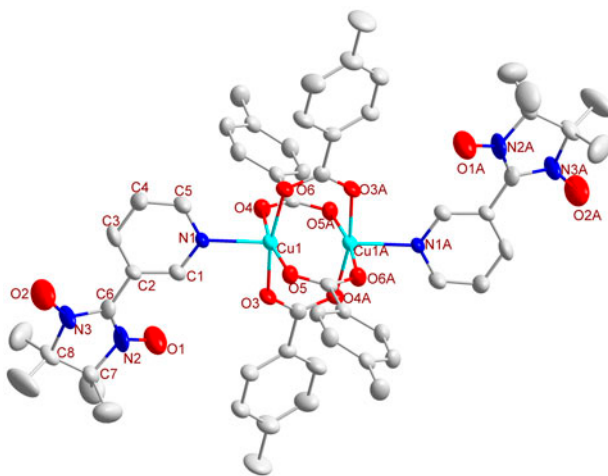


Figure 1(a). ORTEP drawing of $[\text{Cu}_2(4\text{-MePhCOO})_4(\text{NITmPy})_2]$ (**1**) with selected atom-labeling and 30% thermal ellipsoids. All hydrogens are omitted for clarity (symmetry codes: a: $-x+2, -y+2, -z$).

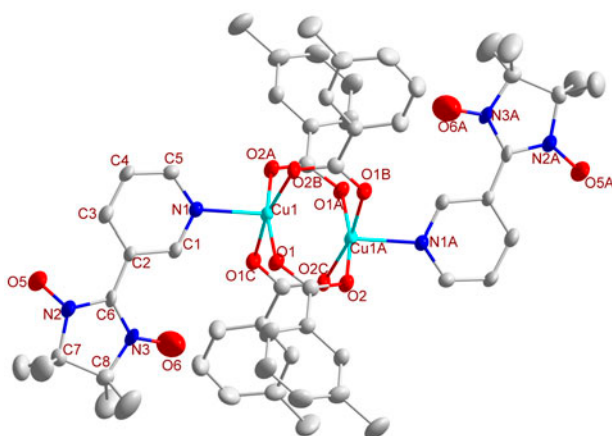


Figure 1(b). ORTEP drawing of $[\text{Cu}_2(3\text{-MePhCOO})_4(\text{NITmPy})_2]$ (**2**) with selected atom-labeling and 30% thermal ellipsoids. All hydrogens are omitted for clarity (symmetry codes: a: $-x+1, -y, -z+1$; b: $-x+1, y, -z+1$; c: $x, -y, z$).

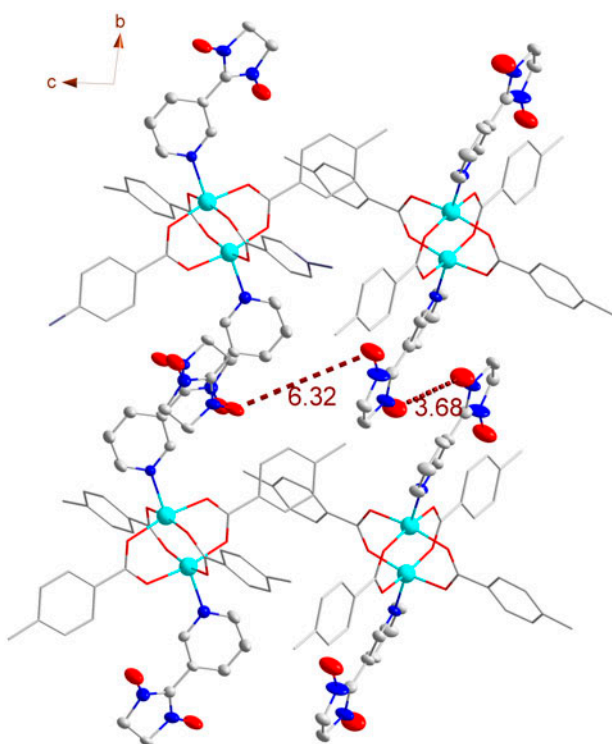


Figure 1(c). The packing plot of **1**, viewed from the a axis, two different orientations in the crystal and the adjacent distance (\AA) of the NITmPy O are shown. For clarity, all hydrogens and methyls of the NITmPy are omitted.

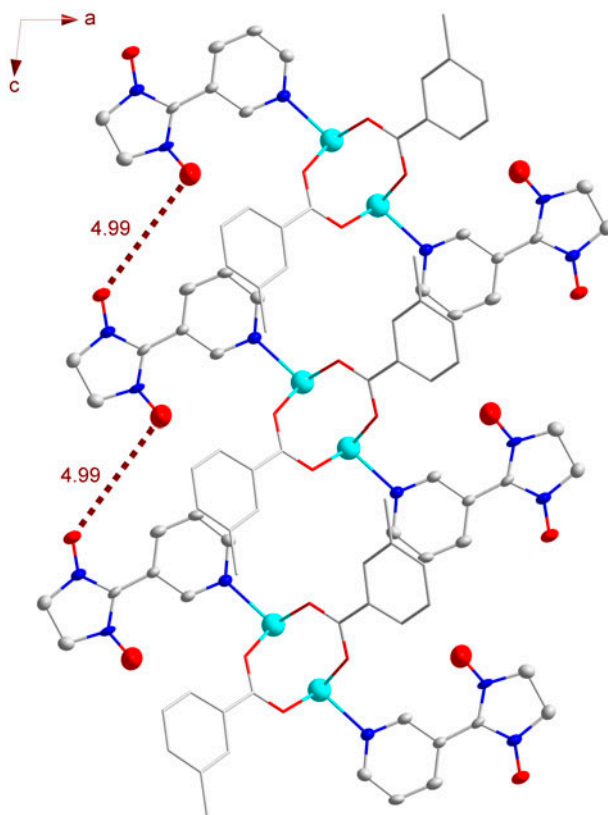


Figure 1(d). The packing plot of **2**, viewed from the *b* axis, the adjacent distance (Å) of the NITmPy O are shown. For clarity, all hydrogens and methyls of the NITmPy are omitted.

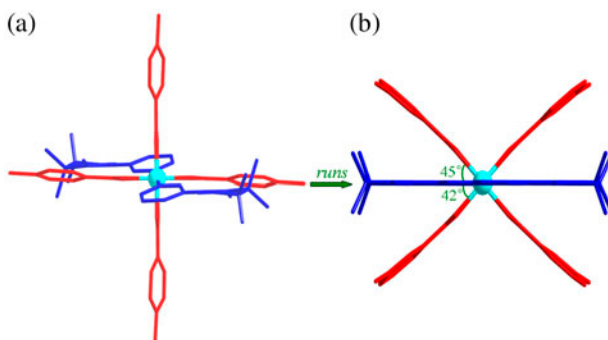


Figure 2. Wires drawing for **1** (a) and **2** (b), viewed from the Cu–Cu axis; NITmPy ligands are shown in blue and fixed on the equatorial position, *p*-toluic acid and *m*-toluic acid are shown in red (see <http://dx.doi.org/10.1080/00206814.2013.800485> for color version).

3.2. PXRD and IR spectra

Purities of samples were confirmed by comparison of experimental and simulated PXRDs (figure S1). The IR spectra of **1** and **2** (figure S2) shows the absorptions of carboxylate

stretch at 1620 cm^{-1} for asymmetric stretch (ν_{as}) and 1400 cm^{-1} for symmetric stretch (ν_{s}) [35]. The absence of strong absorption around 1250 cm^{-1} indicates that all carboxyl groups ($-\text{COOH}$) of toluic ligands are deprotonated [36]. Moreover, bands at 2986 cm^{-1} can be attributed to C–H stretching vibrations. The characteristic absorptions of N–O of the radical should appear at 1360 cm^{-1} , but was covered by the absorption of the strong carboxylate stretch [37].

3.3. Magnetic properties

To analyze exchange coupling in the four spin systems, variable-temperature magnetic-susceptibility measurements were performed on powdered crystalline samples of **1** and **2** in a 1000 Oe field from 2 K–300 K. The obtained data for **1** and **2** are shown as χ_{M} vs. T and $\chi_{\text{M}}T$ vs. T plots in figures 3 and 4, respectively. The χ_{M}^{-1} vs. T plots are shown in supplementary material (figure S3).

According to the data for **1** and **2** of χ_{M}^{-1} vs. T , the magnetic behavior of both complexes follow the Curie–Weiss law $\chi_{\text{M}} = C/(T - \theta)$ from approximately 150 to 300 K, with a Curie constant C value of $2.41\text{ cm}^3\text{ K mol}^{-1}$ and a Weiss temperature θ of -219 K for **1**, and C value of $2.25\text{ cm}^3\text{ K mol}^{-1}$ and a Weiss temperature θ of -245 K for **2**. This behavior is the characteristics of a system with strong antiferromagnetic interactions and magnetic exchange coupling interaction. The χ_{M} vs. T plots of **1** and **2** continuously increase, but no maximum is observed.

For the $\chi_{\text{M}}T$ vs. T curve of **1** (figure 3), $\chi_{\text{M}}T$ is $1.40\text{ cm}^3\text{ mol}^{-1}\text{ K}$ at 300 K, lower than the value ($1.50\text{ cm}^3\text{ mol}^{-1}\text{ K}$) expected for four uncoupled spins of $S = 1/2$ for two nitronyl nitroxide radical ligands and $S = 1/2$ for two copper atoms. Overall, $\chi_{\text{M}}T$ decreases with decreasing temperature, which indicates the existence of antiferromagnetic spin exchange interactions in the dimer. However, when $\chi_{\text{M}}T$ reaches $0.63\text{ cm}^3\text{ mol}^{-1}\text{ K}$ at 24 K, it begins to increase sharply and reaches ca. $0.90\text{ cm}^3\text{ mol}^{-1}\text{ K}$ at 8 K. Then, $\chi_{\text{M}}T$ quickly decreases, finally reaching ca. $0.65\text{ cm}^3\text{ mol}^{-1}\text{ K}$ at 2 K. This behavior indicates the existence of weak ferromagnetic spin exchange interactions in **1**. As shown in figure 4, the $\chi_{\text{M}}T$ of **2** is

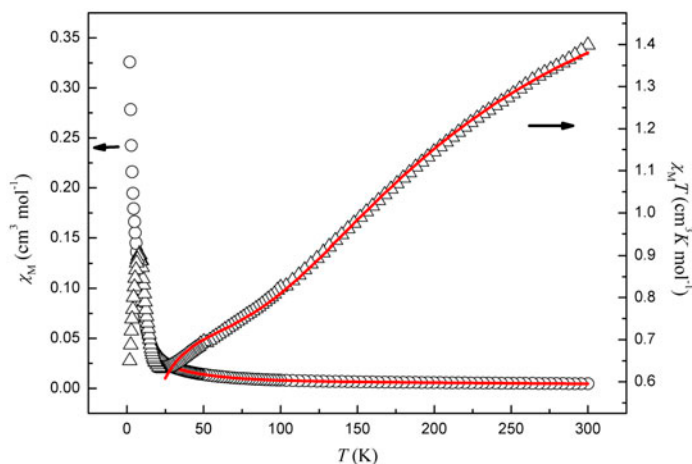


Figure 3. Plots of the temperature dependence of χ_{M} and $\chi_{\text{M}}T$ product at 1 kOe for **1**. The solid lines correspond to theoretical fits.

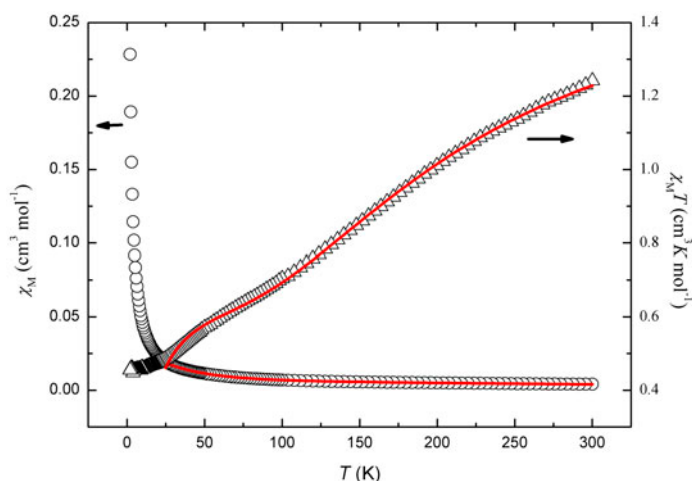


Figure 4. Plots of the temperature dependence of χ_M and $\chi_M T$ product at 1 kOe for **2**. The solid lines correspond to theoretical fits.

$1.24 \text{ cm}^3 \text{ mol}^{-1} \text{ K}$ at 300 K, lower than the expected value ($1.50 \text{ cm}^3 \text{ mol}^{-1} \text{ K}$, similar to **1**). As the system cools from 300 K to 2 K, $\chi_M T$ decreases to ca. $0.45 \text{ cm}^3 \text{ mol}^{-1} \text{ K}$.

The data of **1** and **2** were fitted in several ways. First, we considered the dimer as a centrosymmetric linear tetramer of four $S=1/2$ spins, $S_1-S_2-S_3-S_4$, with the exchange Hamiltonian of $H = -J_1(S_1S_2 + S_3S_4) - J_2S_2S_3 - J_3(S_1S_3 + S_2S_4) - J_4S_1S_4$. Four exchange coupling constants are involved, where S_2 and S_3 refer to Cu^{II} ions, and S_1 and S_4 refer to the nitroxide sites of the NITmPy radicals. However, fitting the magnetic data for the two complexes with this model yielded poor results. Most of the intramolecular exchange path lengths between oxygens of NO groups and Cu^{II} are long, and the spin couplings between the radicals and the Cu^{II} ions are weak. Second, as reported, we considered the system as a strongly coupled dimeric copper unit. The radicals were neglected and the fitting equation $\chi_M = (2Ng^2\beta^2/kT) [3 + \exp(-2J/kT)]^{-1}$ was used, but we still obtained poor results.

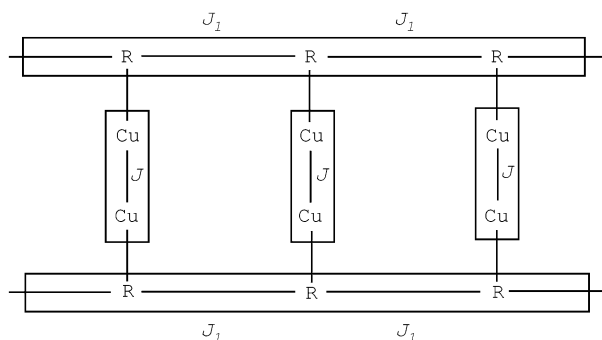
We found that the two complexes have relatively a short contact between the oxygens of N–O (NITmPy) of neighboring dimers. The distances are 3.68 and 6.32 Å for **1** and 4.99 Å for **2**, which indicate that the intermolecular magnetic exchange interaction between NITmPy cannot be neglected. Therefore, the magnetic interaction of the two complexes can be simplified as the exchange coupled Cu–Cu dimer and the radical exchange chain. The model of magnetic interaction in the complexes is shown in scheme 1. The susceptibility data were fitted by the following approximate equations [38, 39]:

$$\chi_M = \chi_{\text{dimer}} + \chi_{\text{chain}}$$

$$\chi_{\text{dimer}} = \frac{2Ng_{\text{Cu}}^2\beta^2}{kT} \times \frac{e^{2J/kT}}{1 + 3e^{2J/kT}}$$

$$\chi_{\text{chain}} = \frac{Ng_R^2\beta^2}{kT} \times \frac{0.25 + 0.074975x + 0.075235x^2}{1 + 0.9931x + 0.172135x^2 + 0.757825x^3}$$

where J is the exchange constant for two Cu^{II} sites, $x = |J_1|/kT$, J_1 is the exchange constant for the radicals, and the other symbols have their typical meanings. The best-fit for **1** is obtained as the solid line (24–300 K) in figure 3. The values of the parameters



Scheme 1. Model of magnetic interaction in the complexes.

are $J = -146.26 \text{ cm}^{-1}$, $g_{\text{Cu}} = 2.35$, $J_1 = -8.71 \text{ cm}^{-1}$, $g_R = 2.94$, and $R = 5.0 \times 10^{-5}$ ($R = \sum (x_M^{\text{calcd}} - x_M^{\text{obsd}})^2 / (x_M^{\text{obsd}})^2$). The best-fit for **2** is obtained as the solid line (24–300 K) in figure 4. The values of the parameters are $J = -147.20 \text{ cm}^{-1}$, $g_{\text{Cu}} = 2.26$, $J_1 = -13.12 \text{ cm}^{-1}$, $g_R = 2.77$, and $R = 5.6 \times 10^{-5}$. The relatively large g_{Cu} values (2.35, 2.26) are similar to the previously reported dimer Cu^{II} carboxylates [32,35,40]. The large negative J of the two complexes indicates strong antiferromagnetic interaction between Cu^{II} ions, and the small negative J_1 suggests weak antiferromagnetic interaction between NITmPy ligands.

In these copper paddle-wheel complexes, nitrogens are located at the apical position in most cases, except for solvent molecules such as water, methanol, or ethanol [41]. Selvakumar *et al.* investigated the strong Cu–Cu interaction and the dinuclear assembly in detail [42]. The $\chi_M T$ vs. T plots of **1** are similar to that of $[\text{Cu}_2(\text{C}_9\text{N}_5\text{H}_9)_2(\text{C}_6\text{H}_5\text{CO}_2)_4]$ [43]. The copper paddle-wheel complexes possess chelate rings and Cu(II) active sites for potential application in host–guest chemistry and catalysis [42]. Moreover, the short distance between the uncoordinated N–O moieties cause more significant intermolecular interactions similar to the lanthanide–radical complexes $[\text{Tb}(\text{hfac})_3(\text{EtVNIT})_2]$ and $[\text{Dy}(\text{hfac})_3(\text{EtVNIT})_2]$, and might exclude the possibility of single-molecule magnet [44].

4. Conclusion

Two new paddle-wheel dimer copper complexes were obtained, and they were structurally and magnetically characterized. Cu^{II} ions are square-pyramidal and short contacts exist between O of the N–O groups of neighboring dimers. Based on the Cu–Cu axis of **1** and **2**, we exploited the steric constraints of the methyl groups and induced the paddle-wheel to run. Two magnetic exchange pathways with strong antiferromagnetic interaction between dimeric Cu ions and weak antiferromagnetic interaction between NITmPy ligands exist in the complexes.

Supplementary material

PXRD graphics, solid state IR spectra, and plots of temperature dependence of χ_M^{-1} of the complexes are available as supplementary material. Crystallographic data for the structural analysis have been deposited with the Cambridge Crystallographic Data Center,

CCDC No. 882654 for **1** and 882653 for **2**. Copies of this information can be obtained free of charge from The Director, CCDC, 12 Union Road, Cambridge, CB2 1EZ, UK (Fax: +44 1223 336 033; E-mail: deposit@ccdc.cam.ac.uk or <http://www.ccdc.cam.ac.uk>).

Acknowledgments

This work was supported by the National Natural Science Foundation of China (Project 21061016) and Yunnan Provincial Department of Education Research Fund (Project 2011Y111).

References

- [1] M.A.S. Aquino. *Coord. Chem. Rev.*, **248**, 1025 (2004).
- [2] N. Schultheiss, C.L. Barnes, E. Bosch. *Cryst. Growth Des.*, **3**, 573 (2003).
- [3] M. Mikuriya, K. Tanaka, M. Handa, I. Hiromitsu, D. Yoshioka, D. Luneau. *Polyhedron*, **24**, 2658 (2005).
- [4] M. Barquín, N. Cocera, M.J. González Garmendia, L. Larrinaga, E. Pinilla, M.R. Torres. *J. Coord. Chem.*, **63**, 2247 (2010).
- [5] Q.Z. Zhang. *J. Coord. Chem.*, **61**, 1849 (2008).
- [6] D.L. Reger, A. Debreczeni, M.D. Smith. *Inorg. Chem.*, **50**, 11754 (2011).
- [7] N. Motokawa, S. Matsunaga, S. Takaishi, H. Miyasaka, M. Yamashita, K.R. Dunbar. *J. Am. Chem. Soc.*, **132**, 11943 (2010).
- [8] M.K.S. Husebye, K. Maartman-Moe, Y. Muto, M. Nakashima, T. Tokii. *Acta Chem. Scand.*, **48**, 628 (1994).
- [9] M. Perec, R. Baggio, R.P. Sartoris, R.C. Santana, O. Peña, R. Calvo. *Inorg. Chem.*, **49**, 695 (2009).
- [10] L.C. Porter, M.H. Dickman, R.J. Doedens. *Inorg. Chem.*, **25**, 678 (1986).
- [11] T. Kawata, H. Uekusa, S. Ohba, T. Furukawa, T. Tokii, Y. Muto, M. Kato. *Acta Cryst. B*, **48**, 253 (1992).
- [12] M. Mikuriya, D. Yoshioka, M. Handa. *Coord. Chem. Rev.*, **250**, 2194 (2006).
- [13] L. Zhu, X. Chen, Q. Zhao, Z. Li, X. Zhang, B. Sun. *Z. Anorg. Allg. Chem.*, **636**, 1441 (2010).
- [14] J.H. Osiecki, E.F. Ullman. *J. Am. Chem. Soc.*, **90**, 1078 (1968).
- [15] E.F. Ullman, J.H. Osiecki, D.G.B. Boocock, R. Darcy. *J. Am. Chem. Soc.*, **94**, 7049 (1972).
- [16] A. Caneschi, D. Gatteschi, J.P. Renard, P. Rey, R. Sessoli. *Inorg. Chem.*, **28**, 3314 (1989).
- [17] K. Jiang, X. Wang, L. Wang, B. Zhao. *J. Coord. Chem.*, **61**, 410 (2008).
- [18] D.Z. Gao, Y.Q. Sun, D.Z. Liao, Z.H. Jiang, S.P. Yan. *J. Coord. Chem.*, **61**, 2413 (2008).
- [19] K. Bernot, L. Bogani, A. Caneschi, D. Gatteschi, R. Sessoli. *J. Am. Chem. Soc.*, **128**, 7947 (2006).
- [20] U. Schatzschneider, T. Weyhermüller, E. Rentschler. *Eur. J. Inorg. Chem.*, **2001**, 2569 (2001).
- [21] L.Y. Wang, C.X. Zhang, D.Z. Liao, Z.H. Jiang, S.P. Yan. *J. Coord. Chem.*, **58**, 969 (2005).
- [22] U. Schatzschneider, T. Weyhermüller, E. Rentschler. *Inorg. Chim. Acta*, **337**, 122 (2002).
- [23] R.S. Drago, Y.Y. Lim. *J. Am. Chem. Soc.*, **93**, 891 (1971).
- [24] H. Tian, R. Liu, X. Wang, P. Yang, Z. Li, L. Li, D. Liao. *Eur. J. Inorg. Chem.*, **2009**, 4498 (2009).
- [25] A. Escuer, M.A.S. Goher, F.A. Mautner, R. Vicente. *Inorg. Chem.*, **39**, 2107 (2000).
- [26] H.Q. Li, X. Zhao, X.C. Hu, G.L. Zhao. *J. Coord. Chem.*, **61**, 3493 (2008).
- [27] R.C. Mehrotra, R. Bohra, D. Gaur. *Metal Carboxylates*, Academic Press, London (1983).
- [28] G.M. Sheldrick. *SHELX-97, Programs for the Solution of Crystal Structures*, University of Göttingen, Göttingen (1997).
- [29] G.M. Sheldrick. *SHELX-97, Programs for the Refinement of Crystal Structures*, University of Göttingen, Göttingen (1997).
- [30] A.W. Addison, T.N. Rao, J. Reedijk, J. van Rijn, G.C. Verschoor. *J. Chem. Soc., Dalton Trans.*, 1349 (1984).
- [31] I. Dasna, S.P. Golhen, L. Ouahab, O. Peña, N. Daro, J.P. Sutter. *New J. Chem.*, **24**, 903 (2000).
- [32] M. Mikuriya, H. Azuma, R. Nukada, Y. Sayama, K. Tanaka, J.W. Lim, M. Handa. *Bull. Chem. Soc. Jpn.*, **73**, 2493 (2000).
- [33] I. Yeltsov, V. Ovcharenko, V. Ikorskii, G. Romanenko, S. Vasilevsky. *Polyhedron*, **20**, 1215 (2001).
- [34] Y.H. Chung, H.H. Wei, G.H. Lee, Y. Wang. *Inorg. Chim. Acta*, **293**, 30 (1999).
- [35] A. Karaliota, O. Kretsi, C. Tzougraki. *J. Inorg. Biochem.*, **84**, 33 (2001).
- [36] K. Nakamoto. *Infrared and Raman Spectra of Inorganic and Coordination Compounds*. p. 64, 6th Edn, Wiley, New York (2009).
- [37] C.X. Zhang, Y. Zhang, C. Cui. *J. Coord. Chem.*, **62**, 2076 (2009).
- [38] O. Kahn. *Molecular Magnetism*. p. 251, VCH, New York (1993).

- [39] Y. Rakitin, V.T. Kalinnikov. *Modern Magnetochemistry*. p. 272, Nauka, Petersburg (1994).
- [40] C. Hadjikostas, G. Katsoulos, M. Sigalas, C. Tsipis, J. Mroziński. *Inorg. Chim. Acta*, **167**, 165 (1990).
- [41] E.M. Rustoy, M. Agotegaray, O.E. Piro, E.E. Castellano. *J. Coord. Chem.*, **65**, 2341 (2012).
- [42] P.M. Selvakumar, E. Suresh, S. Waghmode, P.S. Subramanian. *J. Coord. Chem.*, **64**, 3495 (2011).
- [43] Y.M. Li, C.Y. Xiao, H.R. Feng, S.S. Guo, S.B. Wang. *J. Coord. Chem.*, **65**, 2820 (2012).
- [44] C. Wang, Y.L. Wang, Y. Ma, Q.L. Wang, L.C. Li, D.Z. Liao. *J. Coord. Chem.*, **65**, 2830 (2012).